Journal of Alloys and Compounds 508 (2010) 516–519

Contents lists available at ScienceDirect

Journal of Alloys and Compounds

journal homepage: www.elsevier.com/locate/jallcom

Annealing effects on structural and magnetic properties of Co-doped ZnO nanowires synthesized by an electrodeposition process

Jian-jun Gu[a,b,c], Li-hu Liu[a,b,*], Hai-tao Li[a,b,c], Qin Xu[a,b], Hui-yuan Sun[a,b]

[a] College of Physics Science & Information Engineering, Hebei Normal University, Shijiazhuang 050016, China
[b] Key Laboratory of Advanced Films of Hebei Province, Shijiazhuang 050016, China
[c] Department of Physics, Hebei Chengde Teachers College, Chengde 067000, China

ARTICLE INFO

Article history:
Received 3 March 2010
Received in revised form 5 August 2010
Accepted 18 August 2010

Keywords:
Nanowire
Room-temperature ferromagnetism
Coercivity

ABSTRACT

Arrays of Co-doped ZnO nanowires were fabricated by electrodeposition of Zn^{2+} and Co^{2+} into an anodic aluminum oxide template followed by post-oxidation annealing in an Ar/O_2 mixed atmosphere. Transmission electron microscopy showed that the nanowires were uniform with a diameter of about 75 nm. Significant differences in the crystalline structures of samples annealed at different temperatures were observed. Magnetization measurements showed that the Co-doped ZnO nanowires exhibit room-temperature ferromagnetism that changed with the annealing temperature.

1. Introduction

Recent results have shown that ZnO can serve as a host lattice for transition metal ions thus allowing the creation of new magnetic semiconductor materials [1,2] which may play important roles in future spintronic devices [3,4]. Very recently, various methods have been used to synthesize 1-D Co-doped ZnO nanaowires or nanorods, such as electrochemical process, thermal diffusion and chemical vapour deposition [5–8]. While the nucleation and diffusion process of these methods will cause inhomogeneous distribution of magnetic ions, it is hard to get homogeneous component and high doping products. Hence we focused our work on establishing an easy approach towards the synthesis of homogeneous Co-doped ZnO nanowires by a simple electrodeposition route.

Some researchers have predicted Co-doped ZnO nanaowire is a most promising candidate for room-temperature ferromagnetism [5,9]. Several models have been proposed to explain the magnetic mechanisms, including carrier mediated exchange [10], defect theory [11], and double exchange mechanisms [12].

Compared with bulk and membranous $Co_xZn_{1-x}O$, there have been less experimental studies for the magnetic properties of $Co_xZn_{1-x}O$ nanowires. In this paper, high ordered Co–Zn alloy nanowire arrays had been fabricated in AAO membrane via electrocodeposition process [13,14]. Then the obtained membranes were annealed in an Ar/O_2 mixed atmosphere to make sure that zinc atoms were oxidized to ZnO and the Co^{2+} ions diffused into the lattice of ZnO. Finally, the Co-doped ZnO nanowire arrays were obtained. The structural and magnetic properties of the nanowires were studied in detail.

2. Experimental

Porous anodic aluminum oxide templates were prepared using a two-step anodizing process. Aluminum foils 0.28 mm thick and with purities of 99.999% were anodized for 10 h at 10 °C in 0.3 M oxalic acid solution under a constant potential of 40 V. This process resulted in AAO templates with a pore length of about 40 μm and a nearly uniform diameter of about 75 nm. Afterwards, a 300 nm Cu layer was sputter-deposited onto one side of the AAO template. This layer served as the working electrode for the following electrodeposition process.

The electrolytes for depositing Zn–Co alloy nanowires were prepared from double distilled demineralized water and analytical grade reagents. The sample name and general electrolyte compositions for the as-deposited and post-annealed nanowires are shown in Table 1. It should be noted that the atom ratio of Table 1 was chosen strictly to ensure that the as-deposited nanowires were homogeneous, and does not indicate the Co:Zn ratio in the deposited nanowires. The actual Co:Zn ratio in the nanowires was determined using energy dispersive X-ray spectroscopy (EDS) analysis as described below.

The electrodeposition was carried out in an electrobath at −1.35 V (vs. Hg/HgCl). The temperature of the electrolytes was kept at room temperature and the pH was held at 5.5. The electrodeposition was kept running until deposited CoZn overflowed from the nanoholes. After deposition, the samples were thoroughly washed with demineralized water and ethanol, and dried with hot air. The samples were then annealed in an Ar/O_2 mixed atmosphere with flow rates of 10 sccm O_2 and 240 sccm Ar. Annealing of the samples listed in Table 1 was performed in a quartz tube, holding the nanowire sample temperatures at 400, 500, and 600 °C for 4 h, respectively.

* Corresponding author at: College of Physics Science & Information Engineering, Hebei Normal University, Shijiazhuang 050016, China. Tel.: +86 311 86268312; fax: +86 311 86268314.
E-mail address: lihuliut@126.com (L.-h. Liu).

0925-8388/$ – see front matter © 2010 Elsevier B.V. All rights reserved.
doi:10.1016/j.jallcom.2010.08.107

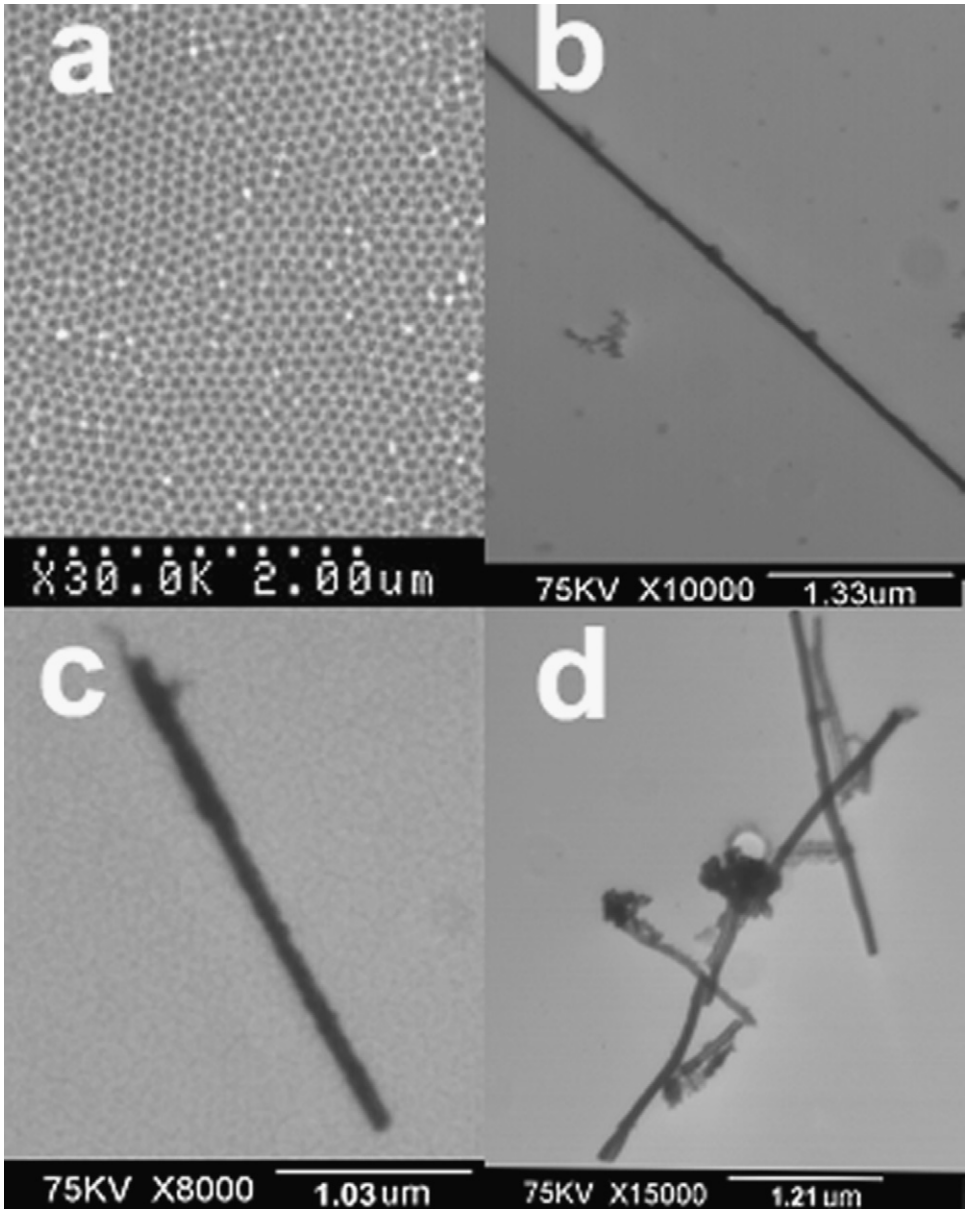

Fig. 1. (a) SEM image of the AAO template with hole diameters of about 75 nm, (b) TEM image of isolated as-deposited Co–Zn nanowires, (c) and (d) isolated nanowire post-annealed at 400 and 500 °C, respectively.

After deposition, the AAO template containing nanowires was dissolved using 5 wt.% NaOH, and washed 3–5 times alternating distilled water and ethanol. The nanowires were then detached from the substrate by ultrasonic dispersion in 2–3 ml of ethanol. A drop of the solution was then placed on a Cu grid with a carbon film and air dried prior to electron microscope analysis.

An Hitachi S-570 field-emission scanning electron microscope (FESEM) and H-600 transmission electron microscope (TEM) were used to study the morphologies of the as-deposited and post-annealed nanomaterials. A Philips X'Pert-MPD x-ray diffractometer (XRD) was employed to determine the different phases and lattice parameters of the nanostructures. The x-ray scan was conducted using Cu-Kα (λ = 1.54056 Å) radiation over a scan range from 20° to 70°. Magnetic measurements were carried out with the Quantum Design Model 6000 vibrating sample magnetometer (VSM) option for the physical property measurement system (PPMS) and parameters like specific saturation magnetization (M_s), coercive force (H_c) and remanence (M_r) were evaluated.

Table 1
Sample name and corresponding synthesizing parameters.

Sample	Annealing temperature (°C)	Electrolyte Ingredients	
a	–	$ZnCl_2$	0.2 M
b	400	$CoCl_2 6H_2O$	0.02 M
c	500	$Na_3C_6H_5O_7 2H_2O$	0.3 M
d	600	KCl	10 g/L
		HBO_3	40 g/L

3. Results and discussion

The FESEM and TEM images of AAO template, as-deposited nanowires and post-annealed nanowires are shown in Fig. 1. From the image of the AAO template (Fig. 1(a)) we can see that the pores have almost identical diameters of 75 nm and spacings of about 25 nm. Fig. 1(b) is a TEM image of an isolated, as-deposited Co–Zn nanowire prepared by electrodeposition for 40 min after removal of the alumina. The diameter of the nanowires is about 75 nm, which corresponds to the pore diameter in the AAO template shown in Fig. 1(a). Fig. 1(c) and (d) is TEM image of nanowires post-annealed at 400 and 500 °C for 4 h with flow rates of 10 sccm O_2 and 240 sccm Ar. It may be seen that the nanowire annealed at 400 °C had a rough surface. Fig. 1(d) shows an even rougher sur-

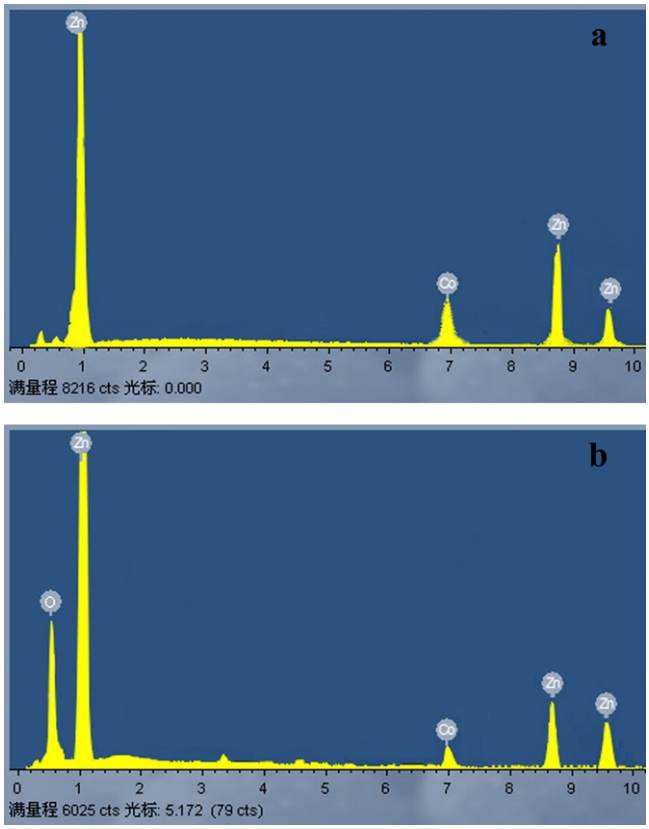

Fig. 2. Typical EDX spectrum taken from individual nanowire of (a) as-deposited and (b) post-annealed at 500 °C.

face on the nanowires annealed at 500 °C. In addition, the lengths of the nanowires annealed at 500 °C are irregular unlike the as-deposited ones. Which can be due to the large mismatch between the thermal expansion coefficient of nanowires and alumina. In the process of annealing, the volume of nanowires can shrink due to the relaxation structure of as-deposited nanowires, and when cooled to room temperature, the nanowires with high aspect ratio contract more than the AAO templates in wire axis, which can produce a break of the originally continuous nanowires.

To precisely define the chemical composition of the nanowires, energy dispersive X-ray spectroscopy (EDS) was used to get the composition of a single nanowire separated from the AAO template. The results are shown in Fig. 2. The Co peak is clearly shown in the EDS spectrum, and the ratio of the areas of the peaks is Zn:Co = 96.2:3.8.

Fig. 3 shows the XRD pattern of the as-deposited Co–Zn alloy nanowires and the nanowires post-annealed in an Ar/O_2 mixed atmosphere at 400 and 500 °C for 4 h. The crystalline structures of the nanowires annealed at different temperatures are significantly different. Fig. 3(a) shows the XRD patterns of the as-deposited Co–Zn alloy nanowires embedded in the AAO template. Only peaks corresponding to Zn (1 0 0) and (1 0 1) orientations (JCPD Card: 001-1238) were observed, showing the absence of a secondary phases, such as zinc oxides or cobalt composites. The crystal structure of the as-deposited Co–Zn alloy nanowires was determined to be a hexagonal structure of P63mmc symmetry.

Fig. 3(b) shows the XRD patterns of the nanowires post-annealed in an Ar/O_2 atmosphere at 400 °C. After annealing, besides the Zn (1 0 1) diffraction peak (denoted by an asterisk in the XRD pattern) from the Zn wurtzite structure, additional peaks from ZnO can be seen. The peaks around 31.8°, 36.4° and 47.7°, which correspond to the peaks of the (1 0 0), (1 0 1) and (1 0 2) planes of the hexagonal

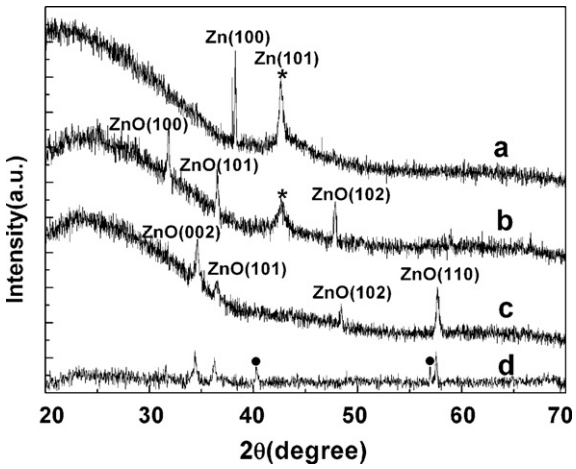

Fig. 3. XRD patterns of aligned Co–Zn nanowires in the AAO template: (a) as-deposited; (b) post-annealed at 400 °C; (c) post-annealed at 500 °C and (d) post-annealed at 600 °C. (*) denotes the Zn peak and (•) denotes the Co oxides peak.

ZnO structure (JCPD Card: 001-1136), indicate the existence of the ZnO phase. However, there is a slight right shift ($\Delta\theta = 0.2°$) of the peaks compared to the standard pattern. The shift may be attributed to the smaller radii of the cobalt ion which decreases the lattice size of the zinc oxide. We can therefore conclude that the Co–Zn alloy of the nanowire has partially transformed into Co-doped ZnO. Fig. 3(c) shows the XRD patterns of the nanowires post-annealed in Ar/O_2 at 500 °C. Compared with the sample annealed at 400 °C, this sample shows only characteristic peaks of ZnO, which suggests that all Zn atoms in the nanowires were oxidized to ZnO and that the Co ions took the place of some of the Zn ions in the ZnO crystal lattice. We can see from this pattern that two new peaks for the (0 0 2) and (1 1 0) planes appear at $2\theta = 34.5°$ and 57.4° in addition to the (1 0 1) and (1 0 2) peaks, which shows that the crystallinity of ZnO is enhanced at the higher annealing temperature. On the other hand, no trace of a second phase or peaks of Zn alone were detected in this pattern. Finally in Fig. 3(d) it may be seen that peaks for CoO (JCPD Card: 042-1300) have appeared suggesting that at least some of the Co has separated from the ZnO lattice and oxidized. The effects of annealing on the structural changes in Co–Zn alloy nanowires may be understood by considering the thermal dynamics. When the zinc in the nanowires was oxidized to ZnO, Co ions could diffuse in the ZnO lattice, resulting in more Co substitution and a more homogeneous distribution in the ZnO matrix. This is consistent with the right shift in peak position observed using XRD in the post-annealed sample.

Fig. 4 shows the magnetic hysteresis loops of the as-deposited and post-annealed nanowires. Measurements were carried out at room temperature with the magnetic field parallel (||) and

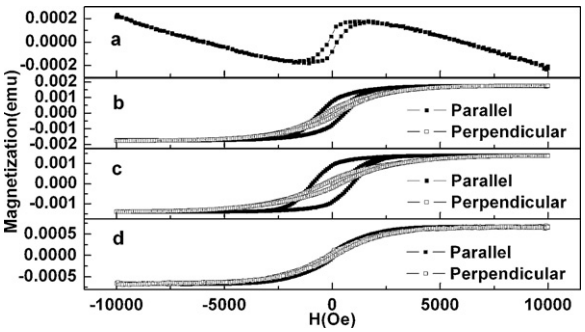

Fig. 4. Magnetic hysteresis loops for nanowires (a) as-deposited and post-annealed at different temperatures of (b) 400 °C,(c) 500 °C and (d) 600 °C, respectively.

perpendicular (⊥) to the long axis of nanowires. The corresponding magnetic fields are designated as $H_{||}$ and $H_{\perp}$, respectively. As-deposited Co–Zn alloy nanowires exhibit soft magnetic behavior with $H_{c||}$ = 100 Oe, as shown in Fig. 4(a), which reflects the intrinsic magnetism of the CoZn alloy nanowires. For the samples annealed at different temperatures, the coercivity (H_c) and remanence (M_r/M_s), which depend on the magnetic anisotropy, first increases with the increasing annealing temperature, amounts to a maximum ($H_{c||}$ = 925 Oe and M_r/M_s = 69%) at 500 °C, and then decreases again with the further increase of annealing temperature. In the whole temperature range, the coercivity of parallel direction is larger than that of perpendicular direction, indicating the effect of shape anisotropy. So the difference of the magnetic hysteresis loops may be attributed to the competition between shape anisotropy and magnetocrystalline anisotropy. For the samples annealed at 400 °C, cobalt will exist as substitutional ions as the oxidation of zinc to ZnO, but the absence of (0 0 2) diffraction peak in Fig. 3(b) indicates a crossover of the orientation of shape anisotropy and magnetocrystalline anisotropy, there by leading to a weak excess coercivity. For the samples annealed at 500 °C, however, a relatively stronger (0 0 2) reflection appears, implying that the primary *hcp* phase with magnetocrystalline easy axis parallel to the wire axis, i.e. the orientation of magnetocrystalline anisotropy is consistent with the one of the shape anisotropy. Then there would be an improvement of coercivity and an additional increasing in the squareness at the nanowires. On the other hand, we can conclude that high-temperature annealing at 600 °C leads to weakened magnetic properties and little magnetic anisotropy from Fig. 4(d), which may be due to the partial of cobalt oxidation to cobalt oxides at higher annealing temperatures (Fig. 3(d)), and which show antiferromagnetism at room temperature. This is an important factor which may affect the magnetism of the nanowires.

The effects of annealing on the magnetic properties of Co-doped ZnO nanowires may be understood by considering the structural changes after each annealing step. It is very likely that a rearrangement of dopants within the nanowires takes place at 400 °C, which helps the system reach the conditions necessary for coupling of the magnetic impurities with a resultant increase in the magnetization. When the sample was annealed at a temperature of 500 °C, more zinc reacted to form the oxide and the preferred orientation changed accordingly, as shown in Fig. 3(c). This enabled the system to reach its optimum condition for increased magnetization. High-temperature annealing at 600 °C, however, may lead to oxidation of cobalt, which is agreement with the XRD result of Fig. 3(d). Hence, the magnetic properties are weakened.

4. Conclusions

In summary, Co-doped ZnO nanowires with diameters of 75 nm were successfully prepared by post-annealing Co–Zn alloy nanowires electrodeposited in AAO templates. It was found that the crystal texture and magnetization of the post-annealed nanowires strongly depended on the annealing temperature. In samples annealed at 400 °C, the as-deposited Co–Zn alloy was partially oxidized to Co-doped ZnO, with a resultant coercivity of H_c = 590 Oe and squareness M_r/M_s = 44%. For samples annealed at 500 °C, the as-deposited nanowires completely changed into Co-doped ZnO, with stronger magnetic properties: H_c = 925 Oe and squareness M_r/M_s = 69%. However, samples annealed at still higher temperatures show weakened magnetic properties.

Acknowledgments

This work has been financed by the Natural Science Foundation of Hebei Province Grant no. A2009000254, the common fund of Hebei Normal University Grant no. L2009Y03 and the Ph.D. fund of Hebei Normal University Grant no. L2006B10. The authors wish to thank Dr. Norman Davison for helpful discussion.

References

[1] T. Miyazaki, S. Yamasaki, Appl. Phys. Lett. 86 (2005) 261910.
[2] T. Agne, Z. Guan, X.M. Li, H. Wolf, T. Wichert, H. Natter, R. Hempelmann, Appl. Phys. Lett. 83 (2003) 1204.
[3] T. Dietl, H. Ohno, F. Matsukura, J. Cibert, D. Ferand, Science 287 (2000) 1019.
[4] Y. Matsumoto, M. Murakami, T. Shono, T. Hasegawa, T. Fukumura, M. Koinuma, Science 291 (2001) 854.
[5] J.B. Cui, U.J. Gibson, Appl. Phys. Lett. 87 (2005) 133108.
[6] T.L. Phan, R. Vincent, D. Cherns, N.H. Dan, S.C. Yu, Appl. Phys. Lett. 93 (2008) 082110.
[7] M. Wei, D. Zhi, J.L. MacManus-Driscoll, Scripta. Mater. 54 (2006) 817.
[8] C.Y. Lin, W.H. Wang, C.S. Lee, K.W. Sun, Y.W. Suen, Appl. Phys. Lett. 94 (2009) 151909.
[9] E.A. Choi, W.J. Lee, K.J. Chang, J. Appl. Phys. 108 (2010) 023904.
[10] A. Walsh, J.L.F. Da Silva, S.H. Wei, Phys. Rev. Lett. 100 (2008) 256401.
[11] W.B. Jian, Z.Y. Wu, R.T. Huang, F.R. Chen, J.J. Kai, C.Y. Wu, S.J. Chiang, M.D. Lan, J.J. Lin, Phys. Rev. B 73 (2006) 233308.
[12] Y.P. Zhang, L.Q. Pan, Mater. Rev 23 (1) (2009) (in Chinese).
[13] J.M. Montero-Moreno, M. Belenguer, M. Sarret, C.M. Muller, Electr. Acta 54 (2009) 2529.
[14] J.H. Gao, Q.F. Zhan, W. He, D.L. Sun, Z.H. Cheng, Appl. Phys. Lett. 86 (2005) 232506.